European Polymer Journal 44 (2008) 3466–3472

Contents lists available at ScienceDirect

European Polymer Journal

journal homepage: www.elsevier.com/locate/europolj

Macromolecular Nanotechnology

Rapid fabrication and formation mechanism of cyclotriphosphazene-containing polymer nanofibers

Jianwei Fu, Xiaobin Huang *, Yan Zhu, Yawen Huang, Lu Zhu, Xiaozhen Tang

School of Chemistry and Chemical Technology, Shanghai Jiao Tong University, 800 Dongchuan Road, Shanghai 200240, China

ARTICLE INFO

Article history:
Received 6 January 2008
Received in revised form 24 July 2008
Accepted 22 August 2008
Available online 30 August 2008

Keywords:
Cyclotriphosphazene
Mechanism
Nanofiber
Self-directing template
Colloid

ABSTRACT

Cyclotriphosphazene-containing polymer nanofibers with uniform diameters, high aspect ratios, and high specific surface area have been synthesized rapidly at high yields under ultrasonic irradiation *via* a self-directing template approach. During the polymerization, triethylamine (TEA) as an acid acceptor absorbed a byproduct hydrogen chloride (HCl) to afford triethylamine hydrochloride (TEACl), acting as structure-directing template and guiding the formation of nanofibrous structures. The mechanism was confirmed by means of SEM, TEM, FTIR, XRD, TG, and N_2 adsorption method. The molecular structure of as-synthesized polymer nanofibers was characterized by solid state NMR and elemental analysis.

1. Introduction

Nanosized materials are receiving great technological and scientific interest due to their unique physicochemical properties different from those of conventional bulk materials. Several nanosized materials such as nanotubes, nanowires, nanofibers, nanorods, nanobelts, nanocombs, nanocrystals, nanospheres, and nanocapsules are currently under investigation for various high technology applications [1–4]. Among them, polymer nanofibers are of particular importance, owning to their intriguing properties such as diverse functionality, flexibility, tunable surface characteristics, and increased specific surface area. Additionally, polymer nanofibers have many potential applications, such as in molecular devices [5], optics [6], sensors [7], carriers [8], and tissue engineering materials [9,10]. To date, several fabrication techniques are being investigated to develop polymer nanofibers. These include template synthesis [11], drawing [12], phase separation [13], self-assembly [14,15], and electrospinning [16–18]. However, from a materials point of view, a rapid synthesis of pure and uniform polymer nanofibers is still a major challenge for materials scientists under milder conditions.

Hexachlorocyclotriphosphazene (HCCP) is a cyclic inorganic compound formed by three —P=N— units and six chlorine substitutes. The high reactivity of these substitutes offers the possibility to build up polymers with interesting properties. In past decades, a series of cyclotriphosphazene-containing polymers have been reported, and they are used in flame-retardant materials [19,20], thermoset resins [21,22], electrolytes [23], biomaterials [24,25], and so on.

In this article, we present an approach to uniform cyclotriphosphazene-containing polymer nanofibers by polycondensation of HCCP and 4,4′-sulfonyldiphenol in the presence of triethylamine. The advantage of the approach includes simplicity, rapidity, low cost, ease of scale-up, and good reproducibility. Gram-scale products can be obtained that contained almost exclusively cyclotriphosphazene-containing polymer nanofibers. At the same time, we tracked the obvious morphological changes of the nanofibers with increasing reaction time and proposed their formation mechanism – self-directing template

* Corresponding author. Tel.: +86 21 54747142; fax: +86 21 54741297.
E-mail address: fjwhnhx@sjtu.edu.cn (X. Huang).

0014-3057/$ - see front matter © 2008 Elsevier Ltd. All rights reserved.
doi:10.1016/j.eurpolymj.2008.08.026

approach. This study might offer important insights into the synthesis of other polymer nanostructures.

2. Experimental section

2.1. Raw materials

HCCP (synthesized as described in the literature [26]) was recrystallized from dry hexane followed by sublimation (60 °C, 0.05 mm Hg) twice before use (mp = 112.5–113 °C). 4,4′-Sulfonyldiphenol (BPS) (purify > 99.5%) was obtained from Jiangsu Alonda High-Tech Industry Co., Ltd. (Jiangsu, China) and used as received. Acetone and triethylamine (TEA) was purchased from Shanghai Chemical Reagents Corp. (Shanghai, China) and used without further purification.

2.2. Synthesis

The rapid preparation of poly(cyclotriphosphazene-4,4′-sulfonyldiphenol) (PZS) nanofibers was carried out as follows (Scheme 1). TEA (0.71 g, 7.02 mmol) was added to a solution of HCCP (0.27 g, 0.78 mmol) and BPS (0.59 g, 2.34 mmol) in acetone (50 mL). The reaction mixtures were stirred in an ultrasonic bath (40 kHz, 50 W) at 7 °C for 10 min. The gel-like solid produced was washed four times using acetone and de-ionized water, respectively. Finally, the resulting product was dried under vacuum to yield PZS nanofibers as a hard white agglomeration. Synthesis yield was about 75 wt%, calculated from HCCP.

2.3. Characterization

The morphologies of PZS nanofibers were observed by scanning electron microscopy (SEM, JEOL JSM-7401F) and transmission electron microscope (TEM, JOEL JEM-100CX). The surface area of the nanofibers was measured by nitrogen adsorption–desorption isotherms using the Brunauer–Emmett–Teller (BET) method (Belsorp-mini). The molecular structure of PZS nanofibers was characterized by a Perkin-Elmer Paragon 1000 Fourier transform spectrometer (FTIR) at room temperature (25 °C). X-ray diffraction (XRD) patterns were recorded by using a Bruker D8 Advance instrument equipped with Cu Kα radiation performed at 40 kV and 40 mA. A Perkin Elmer TGA 7/DX thermogravimetric analyzer was used to investigate the thermal stability of the PZS nanofibers at a heating rate of 10 °C min^{-1} under nitrogen atmosphere. Elemental analyses (EA) were performed using a Perkin Elmer 2400. Nuclear magnetic resonance spectra of ^{13}C and ^{31}P using the cross-polarization magic angels spinning (CP-MAS) technique were measured in a Varian Mercury Plus 400 (Varian, USA) spectrophotometer.

3. Results and discussion

Fig. 1a showed SEM images of bulk and uniform PZS nanofibers synthesized *via* a self-directing template route. As one can see, all PZS samples obtained in the method were fibrous with a diameter of 40–60 nm and length up to several thousand nanometers. A close look at the nanofibers revealed that their surface was rather rough with some nanoparticles with an average of several nanometers as shown in Fig. 1b. The coarse texture was favor of the increase of the surface area of the PZS nanofibers, which had been proved by N_2 adsorption test. The results showed that BET surface area of the PZS nanofibers was 79.3 $m^2 g^{-1}$, which was far greater than that of HCl dedoped polyaniline nanofibers (average diameter = 30 nm, 54.6 $m^2 g^{-1}$) with relative smooth surface reported by Huang and co-workers [27]. The rough texture could help better know the formation mechanism of the nanofibers. Of course, from the application point of view, the special structure also indicated that the PZS nanofibers had a potential for absorbing materials.

Fig. 1c and d showed TEM images of the PZS nanofibers which further confirmed their fibrillar morphology. The diameters and lengths of them were consistent with those shown in Fig. 1a and b. After observing the TEM images carefully, we could find that the PZS nanofibers were solid and every nanofiber was assembled by large amounts of nano-scale particles along its axes (shown in Fig. 1d).

In order to investigate the formation mechanism of PZS nanofibers, we decided to track the morphological evolution of PZS during condensation polymerization. The PZS products were sampled periodically with a syringe from the reaction bath for examination under an electron microscope. To avoid the formation of new *ex situ* PZS, the polymerization needed to be quenched as soon as possible. Therefore, special care had to be taken by quickly depositing the reaction extract onto a glass slice or a copper net under infrared lamp for SEM or TEM observation.

The SEM images of the product at different reaction stages are shown in Fig. 2. At a very early stage of the polymerization process, a mass of irregularly shaped nanoparticles – polymer colloids (shown in Fig. 2a) were obtained.

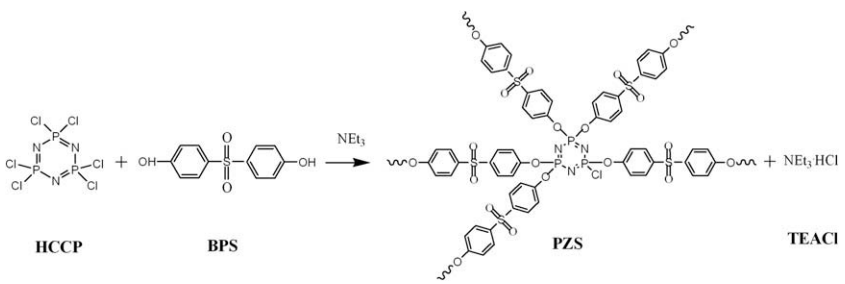

Scheme 1. Synthesis of the highly cross-linked PZS nanofibers.

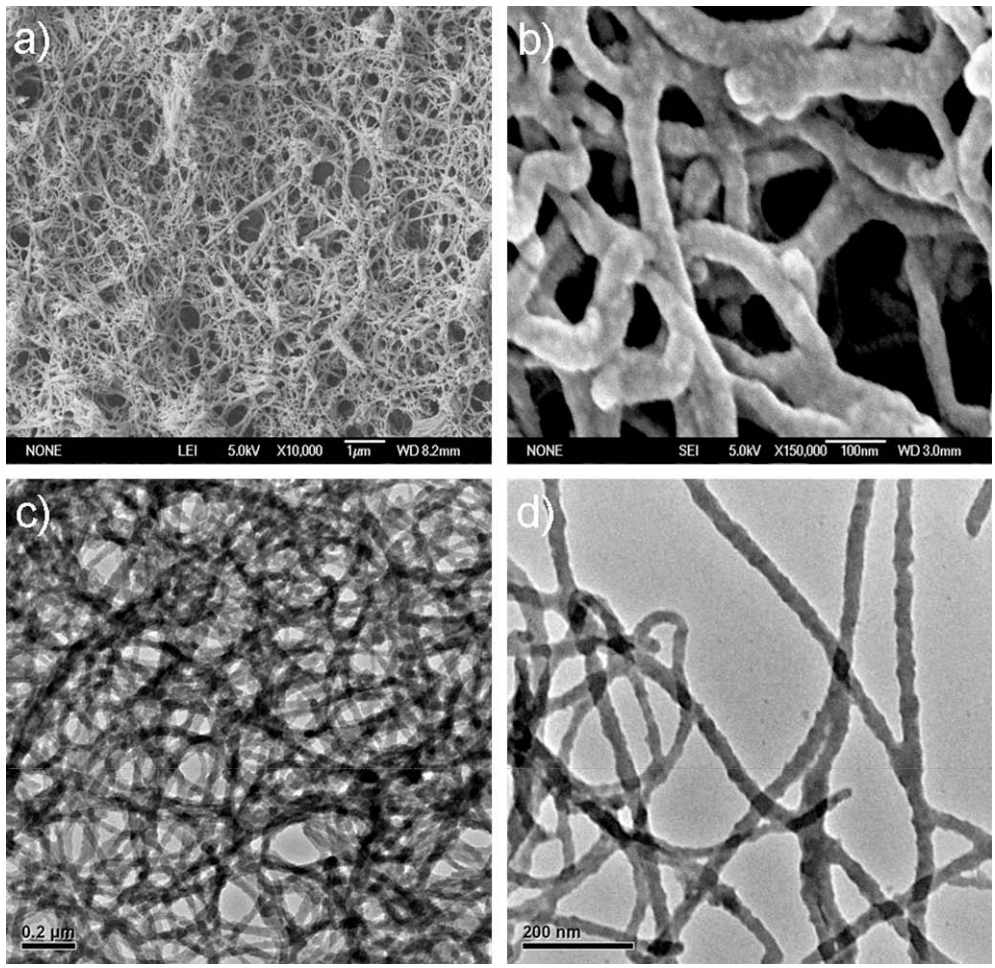

Fig. 1. (a and b) Field-emission SEM images of the PZS nanofibers. (c and d) HR-TEM images of the PZS nanofibers.

As the reaction was carried out, a visible protuberance derived from a colloid aggregate (shown in Fig. 2b, inset), then the protuberance prolonged gradually (shown in Fig. 2c) and formed nanofibers finally (shown in Fig. 2d and e). In addition, Fig. 2f showed a high resolution TEM image of the product at middle reaction stage. A typical oriented attachment of colloid aggregates were clearly recognized, which could also help to know the formation mechanism of nanofibers.

The SEM results showed that the polycondensation could finish in a rather short period such as 8 min, which was advantageous for multiple preparations of nanofibers rapidly. Additionally, the results also indicated that the protuberance played an important role in the formation of PZS nanofibers. Then what the protuberance was?

To address the question, we should consider the polymerization process. Polycondensation was carried out in a solution of acetone with excess TEA as an acid acceptor. Under ultrasonic irradiation, the polymerization of HCCP with equimolar BPS generated uneven nanometer-sized polymer colloids and hydrogen chloride (HCl). Triethylamine absorbed the HCl to afford TEACl, which accelerated the polymerization. As ion crystals, TEACl had rather high surface energy, whereas organic polymers had relatively low surface energies (under 100 mN m^{-1}) [28,29]. As a rule, materials with low surface energies could spontaneously spread over the substances with higher surface energies. One typical example based on this rule was the preparation of nanotubes by template wetting [30]. Therefore, TEACl could be adhered by the polymer colloids and formed large amounts of colloid aggregates. At the same time, the growing trend of TEACl along its axes guided the oriented attachment of these colloid aggregates (shown in Fig. 2f). The further cross-linking of colloids was also carried out with the reaction progressing. Thus, nanofibers could undergo a process from polymer colloids (Fig. 2a) to colloid aggregates (Fig. 2b), short nanorods (Fig. 2c), and long nanofibers (Fig. 2d and e). Therefore, we thought the protuberance was just the growing TEACl nanocrystal which was covered with polymer colloids. During the polymerization, the TEA nanocrystal produced *in situ* played a role of directing template, guiding the growth and formation of PZS nanofibrous structures. Because of the rapid polymerization process, the discontinuous TEACl template was small in bulk. As soon as it was removed, the room left by the template was easily eliminated because of the inherent flexibility of polymer colloids. So, the final nanofibers were solid.

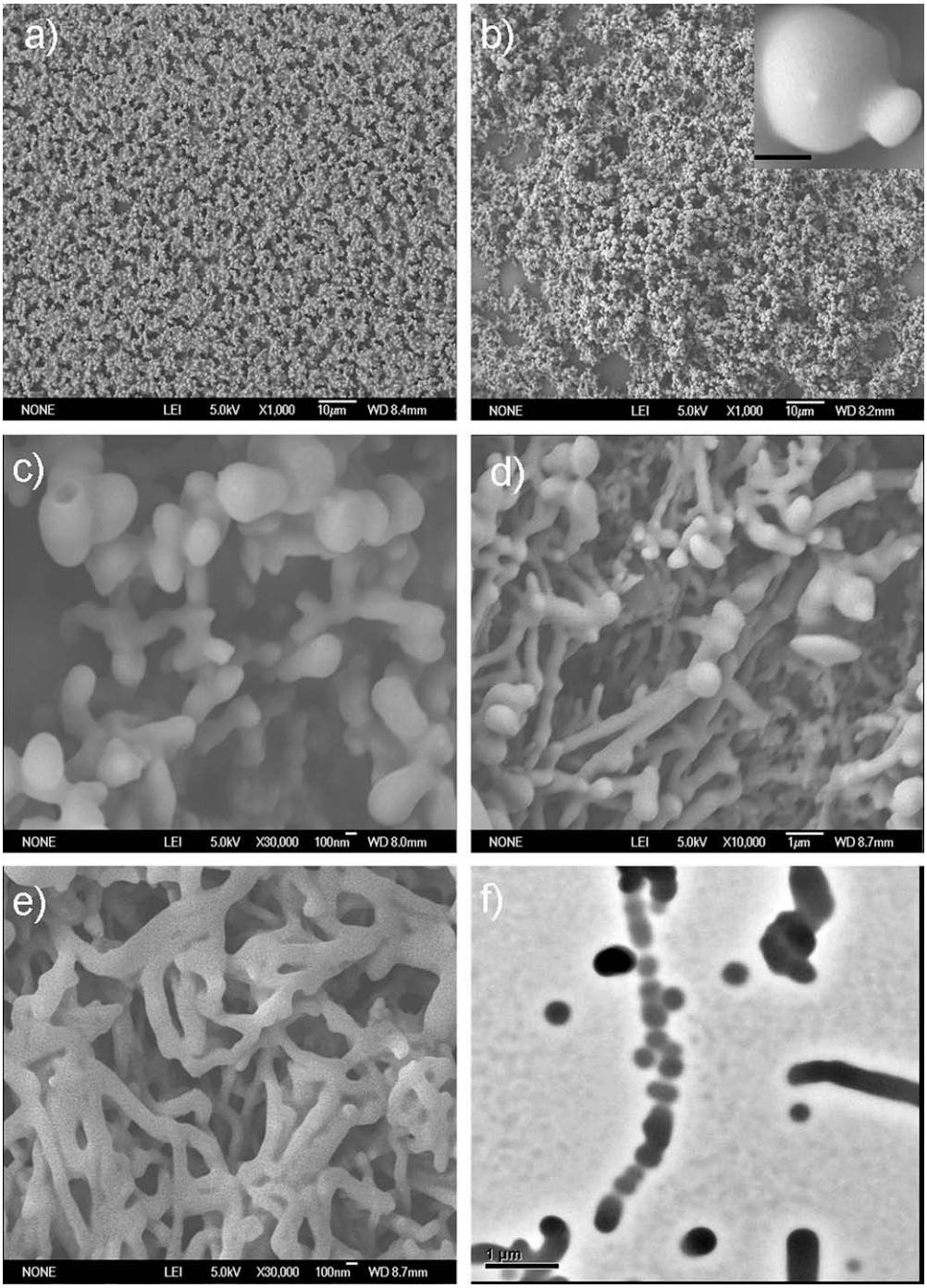

Fig. 2. SEM (a–e) and TEM (f) images showing the morphological evolution process of PZS from sphere-like colloids to nanofibers as the reaction proceeds. The reaction times are (a) 1, (b) 2.5, (c) 4, (d) 5, (e) 8, (f) 4 min, respectively. Time 0 was defined as the moment that TEA was added to the reaction solution. Samples (a–f) were extracted form the reaction bath and deposited immediately onto a glass slice or copper net under an infrared lamp. The inset in (b) showed the magnified image of one PZS colloid aggregate with protuberance (scale bar = 100 nm).

Predictably, if the speed of polymerization was slow enough and the TEACl nanocrystal as directing template had time enough to grow along its axes in a special condition, core/shell structure could be formed. As soon as the core was removed, a novel nanotubular structure would be obtained. In fact, this possibility could truly occur and we had proved in our previous study [31].

Based on the analysis of morphological evolution, we proposed a formation mechanism of PZS nanofibers which could be schematically expressed using Fig. 3. To verify the

validity of our proposed mechanism, we must prove the directing template was truly present in the middle of PZS nanofibers – Compound **1**. Therefore, a series of experiments had been done as shown below.

Spectroscopically, a number of characteristic absorptions of Compound **2** were observed (shown in Fig. 4), such as the phenylene absorption of sulfonyldiphenol units at 1591 and 1490 cm^{-1}, the O=S=O stretching vibration at 1294 and 1154 cm^{-1}, the absorption of cyclotriphosphazene at 1187 and 880 cm^{-1}, and the absorption of P—O—(Ph) at 941 cm^{-1}, which were evidences showing the condensation of monomers HCCP and BPS. In addition, the strong absorption peak of —OH at 3400 cm^{-1} in monomer BPS disappeared in Compound **1** after reaction, which further confirmed the occurrence of polymerization. It was worthy of notice that the peaks at 2976, 2939, and 2678 cm^{-1} in Compound **1**, which were assigned to the C—H asymmetrical stretching vibration of the methyl groups, methene groups and the N^{+}—H stretching vibration of the tertiary amine salt, were the significant evidences to prove the existence of TEACl. XRD for Compounds 1 and 2 were also measured to further confirm this result. As shown in Fig. 5, it was obvious that Compound **1** was mixtures of amorphous and crystalline materials while Compound **2** was amorphous. Moreover, the X-ray diffraction pattern of Compound **1** (shown in Fig. 5) could be readily indexed to TEACl with a calculated lattice constant of $a = 8.740$ Å, which was in consistent with the standard value (JCPD file 38-1974). The same result could be found in TG analysis, as shown in Fig. 6. There was significant difference between Compounds 1 and **2**. The onset of the thermal-degradation temperature of Compound **2** was 444 °C, while that of Compound **1** was 187 and 448 °C, respectively. The results also suggested that the onset of the thermal-degradation temperature of TEACl in Compound **1** was 187 °C and Compound **2** had better thermal stability.

In addition, the molecular structure of Compound **2** was confirmed by solid state NMR and elemental analysis. Fig. 7a showed ^{13}C cross-polarization magic angle spinning (CP MAS) NMR and quantitative solid state ^{31}P NMR spectra of Compound **2**. The ^{13}C NMR spectrum showed

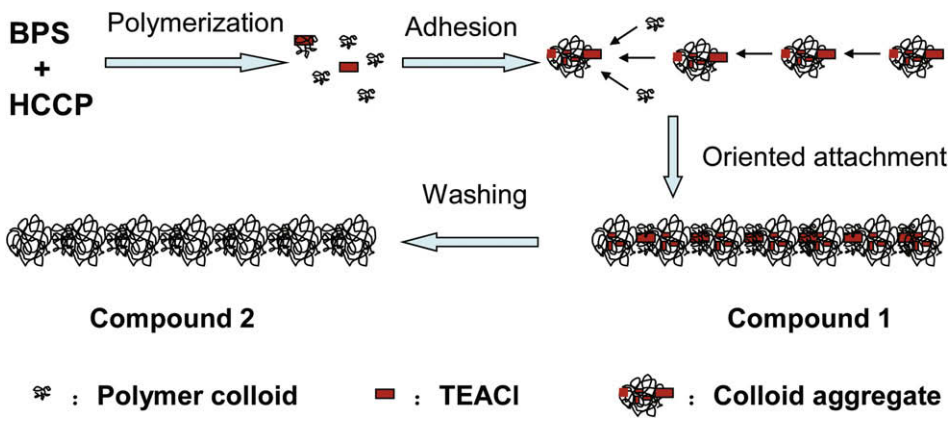

Fig. 3. Schematic illustration of the procedure for the synthesis of the PZS nanofibers *via* a self-directing template approach.

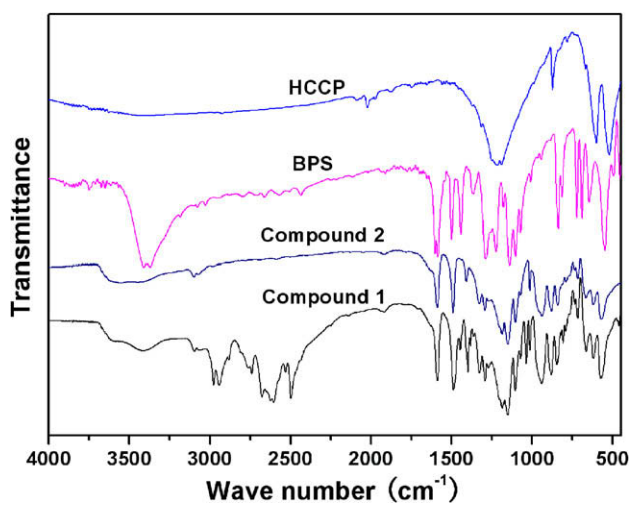

Fig. 4. Infrared spectra of BPS, HCCP, Compounds **1** and **2**. Compounds **1** and **2** were the PZS nanofibers before and after washing with de-ionized water, respectively.

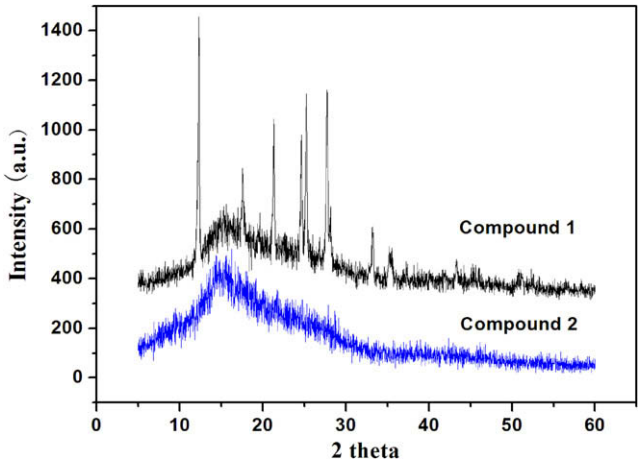

Fig. 5. X-ray diffraction patterns of Compounds **1** and **2**. Compounds **1** and **2** were the PZS nanofibers before and after washing with de-ionized water, respectively.

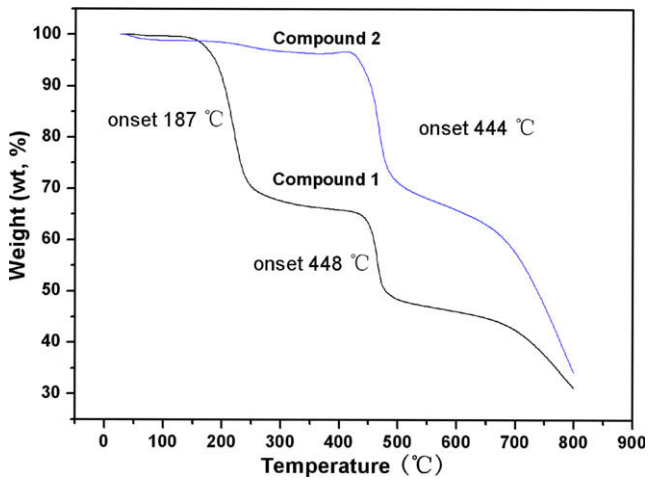

Fig. 6. TGcurves of Compounds **1** and **2**. Compounds **1** and **2** were the PZS nanofibers before and after washing with de-ionized water, respectively.

phenylene group at 153, 139, 129, and 121 ppm. Since resonance of the phenylene carbon bearing a hydroxyl group in BPS was not detected at 161 ppm, it can be concluded that the two hydroxyl groups of each BPS have reacted with HCCP completely. There were two signals appeared at 3 and 20 ppm in the quantitative ^{31}P NMR spectrum of the PZS nanofibers with an area ratio of 1:2, indicating the presence of —N=P(—$(OPh)_2$)— and —N=P(—OPh)(—Cl)—, respectively. The minor peak at 20 ppm is assigned to the unit with a P–Cl bond, thus, about one third of the phosphorus atoms existed in the form of —N=P(—OPh)(—Cl)— in the Compound **2**. The fraction of P—Cl groups unreacted could be attributed to the steric hindrance.

The elemental analysis of Compound **2** gave the following results. Calcd for $C_{30}H_{20}ClN_3O_{10}P_3S_{25}$ (PZS): C, 45.5; H, 2.5; Cl, 4.5; N, 5.3; P, 11.8; S, 10.1. Found: C, 45.1; H, 2.7; Cl, 6.2; N, 5.4; P, 12.0; S, 10.0.

Based on FTIR, EA and NMR analysis, we can predicate that the molecular structure of Compound **2** was highly cross-linked networks, as shown in Fig. 7b.

4. Conclusions

This work has demonstrated the cyclotriphosphazene-containing polymer nanofibers can be fabricated rapidly *via* self-directing template approach, which will make industrialization of these nanostructures easy and inexpensive. Scanning electron microscope was used to track the obvious morphological evolution process of PZS products with the increasing reaction time. The results showed that the nanofiber morphology experienced a series of changes, including nanosized polymer colloids, colloid aggregates, short nanorods, and long nanofibers. During the process, the TEACl nanocrystals formed *in situ* played key roles of self-directing template, guiding the formation of nanofibrous structure. SEM, TEM, FTIR, XRD, TG, solid state NMR, EA, and N_2 adsorption method confirmed the formation mechanism. In addition, the highly cross-linked molecular structure of as-synthesized PZS nanofibers was also confirmed by solid state NMR and EA. The finding could inspire creative imagination to design new system

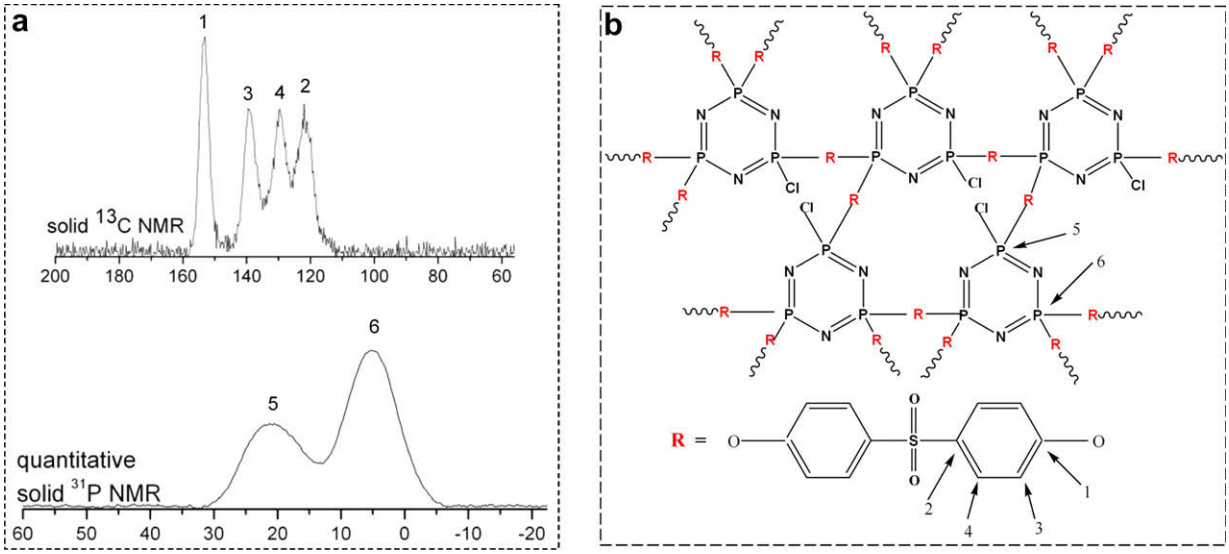

Fig. 7. (a) Solid state ^{13}C and quantitative solid state ^{31}P NMR spectra of Compound **2**. (b) Highly cross-linked molecular structure of Compound **2**. Compound **2** was the PZS nanofibers after washing with de-ionized water.

and orchestrate particular shape and morphology of micro- and nanostructures.

References

[1] Holmes JD, Johnston KP, Doty RC, Korgel BA. Science 2000;287:1471–3.
[2] Ge JP, Li YD. Adv Funct Mater 2004;14:157–62.
[3] Yu DB, Yu SH, Zhang SY, Zuo J, Wang DB, Qian YT. Adv Funct Mater 2003;13:497–505.
[4] Chen JY, Wiley BJ, Xia YN. Langmuir 2007;23:4120–9.
[5] Aleshin AN. Adv Mater 2006;18:17–27.
[6] Babel A, Li D, Xia YN, Jenekhe SA. Macromolecules 2005;38:4705–11.
[7] Huang JX, Virji S, Weiller BH, Kaner RB. Chem Eur J 2004;10:1314–9.
[8] Ko S, Jang J. Biomacromolecules 2007;8:1400–3.
[9] Pham QP, Sharma U, Mikos AG. Biomacromolecules 2006;7:2796–805.
[10] Yang F, Murugan R, Wang S, Ramakrishn S. Biomaterials 2005;26:2603–10.
[11] Martin CR. Chem Mater 1996;8:1739–46.
[12] Ondarcuhu T, Joachim C. Europhys Lett 1998;42:215–20.
[13] Ma PX, Zhang RY. J Biomed Mater Res 1999;46:60–72.
[14] Whitesides GM, Grzybowski B. Science 2002;295:2418–21.
[15] de Moel K, Alberda van Ekenstein GOR, Nijland H, Polushkin E, ten Brinke G, Maki-Ontto R, et al. Chem Mater 2001;13:4580–3.
[16] Huang ZM, Zhang YZ, Kotaki M, Ramakrishna S. Sci Technol 2003;63:2223–53.
[17] Catalani LH, Collins G, Jaffe M. Macromolecules 2007;40:1693–7.
[18] Chronakis IS. J Mater Process Technol 2005;167:283–93.
[19] Chen-Yang YW, Yuan CY, Li CH, Yang HC. J Appl Polym Sci 2003;90:1357–64.
[20] Yuan CY, Chen SY, Tsai CH, Chiu YS, Chen-Yang YW. Polym Adv Technol 2005;16:393–9.
[21] Luther TA, Stewart FF, Lash RP, Wey JE, Harrup MK. J Appl Polym Sci 2001;82:3439–46.
[22] Mathew D, Reghunadhan Nair CP, Ninan KN. Polym Int 2000;49:48–56.
[23] Kaskhedikar N, Burjanadze M, Karatas Y, Wiemhöfer HD. Solid State Ionics 2006;177:3129–34.
[24] Yuan WZ, Yuan JY, Huang XB, Tang XZ. J Appl Polym Sci 2007;104:2310–7.
[25] Cui YJ, Tang XZ, Huang XB, Chen Y. Biomacromolecules 2003;4:1491–4.
[26] De Jaeger R, Gleria M. Prog Polym Sci 1998;23:179–276.
[27] Huang JX, Kaner RB. J Am Chem Soc 2004;126:851–5.
[28] Fox HW, Hare EF, Zisman WA. J Phys Chem 1955;59:1097–106.
[29] Wu S. Polymer blends. In: Paul DR, Newman S, editor. New York: Academic Press; 1978. p. 244–88.
[30] Steinhart M, Wehrspohn RB, GÖsele U, Wendorff JH. Angew Chem Int Ed 2004;43:1334–44.
[31] Zhu L, Xu YY, Yuan WZ, Xi JY, Huang XB, Tang XZ, et al. Adv Mater 2006;18:2997–3000.